Werk

Jahr: 1978
Kollektion: fid.geo
Signatur: 8 Z NAT 2148:45
Digitalisiert: Niedersächsische Staats- und Universitätsbibliothek Göttingen
Werk Id: PPN1015067948_0045
PURL: http://resolver.sub.uni-goettingen.de/purl?PPN1015067948_0045

LOG Id: LOG_0059
LOG Titel: Reinterpretation of a deep-seismic-sounding profile on the Ukrainian shield
LOG Typ: article

Übergeordnetes Werk

Werk Id: PPN1015067948
PURL: http://resolver.sub.uni-goettingen.de/purl?PPN1015067948
OPAC: http://opac.sub.uni-goettingen.de/DB=1/PPN?PPN=1015067948

Contact

Niedersächsische Staats- und Universitätsbibliothek Göttingen
Georg-August-Universität Göttingen
Platz der Göttinger Sieben 1
37073 Göttingen
Germany
Email: gdz@sub.uni-goettingen.de

J. Geophys. 45, 355–372, 1979

Journal of Geophysics

Reinterpretation of a Deep-Seismic-Sounding Profile on the Ukrainian Shield*

M. Jentsch

Geophysikalisches Institut der Universität Karlsruhe,
Hertzstr. 16, D-7500 Karlsruhe 21, Federal Republic of Germany

Abstract. A single deep-seismic-sounding profile from the Ukrainian shield has been reinterpreted. The spacing of geophone traces in the original data was 100 m. The data are presented with 200 m, 1 km and 3 km distance between traces to allow a comparison with the type of explosion seismic data common in Western Europe and North America. Different possible correlations are presented and discussed. The DSS data have been interpreted using conventional techniques for laterally homogeneous models, i.e., traveltime modelling and synthetic seismograms. No decision can be made over the possible existence of a low velocity zone in the middle or lower crust. Two one-dimensional velocity-depth functions are derived. They include a high-velocity layer beneath the crust-mantle boundary, introduced to explain strong amplitudes at rather short shotpoint distances. These results are compared with earlier interpretations of this profile.

Key words: Deep-seismic-sounding – Traveltimes – Synthetic seismograms – Correlation.

Introduction

The Ukrainian shield is bordered by the Dnjepr-Donetz-Depression in the north and the Crimean Highlands and the Black-Sea-Depression in the south. It forms the core of the ancient East-European Platform where mountain systems existed in the early Proterozoic. The roots of these mountains are still present today and form a crust of 30–60 km thickness (Sollogub et al., 1973a).

To obtain a better understanding of the area a number of seismic measurements were undertaken during the last decade (Sollogub et al., 1973b). From the *Deep-Seismic-Sounding* (DSS) profile No. 10, situated on the extreme eastern part of the shield, the first 135 km of observations from shotpoint 0.0 (Fig. 1)

* Contribution no. 157, Geophysical Institute, University of Karlsruhe. – This paper was presented at the CCSS-workshop on comparative interpretation of explosion seismic data in Karlsruhe in August 1977

0340-062X/79/0045/0355/$03.60

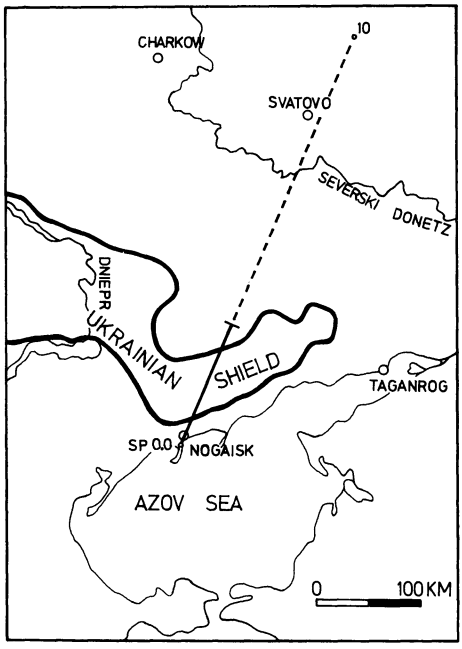

Fig. 1. Position of the USSR national profile No. 10 Nogaisk-Svatovo. *Solid line*: part of profile No. 10 covered by shot 0.0. *Stippled line*: part of profile No. 10 not available in this interpretation

are reinterpreted in this paper. The technique of DSS was developed during the 1950's and 60's from seismic prospecting methods used in the USSR (Kosminskaya, 1971). Since high frequencies and seismometer spacing of 100–200 m are used, correlations can be made quite easily and many seismic phases can be identified on typical DSS-record sections, many of them with only limited horizontal persistence. The published interpretations of profile No. 10 were presented in 2-dimensional cross-sections with contours of iso-velocity. In this paper conventional one-dimensional methods based on assumptions of lateral homogeneity have been applied to the DSS-data. These methods were developed for the interpretation of explosion seismic data with a mean seismometer spacing of 3–5 km. To illustrate the difference between the very close and wider spaced data and the resulting effects on correlation and information content record sections were plotted with different spacing of traces. Another purpose of this work was to show to what extent it might be useful to use amplitudes in a high frequency crustal study.

A comparison between the two-dimensional interpretations of Pavlenkova (1971) and Pavlenkova and Smelyanskaya (1970) and the joint traveltime and amplitude interpretation described in this paper indicates that the main features of the crustal structure appear in both types of models although a lot of information was missing for the interpretation presented here, e.g., reversed profiles, exact position of the shotpoint, setting of instruments etc.

The Data

The data available were photographic copies of the original recordings (Fig. 2). On every trace the shotpoint-receiver distance was indicated together with time

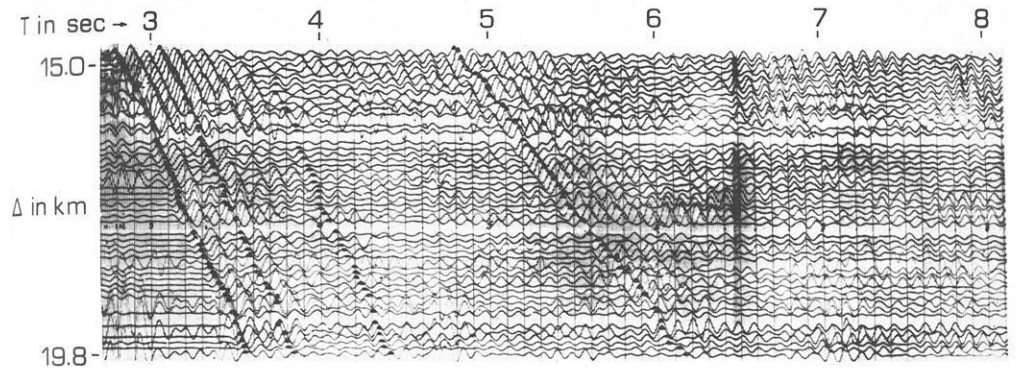

Fig. 2. Photographic copy of the original data. Distance Δ in Kilometer, time in seconds from the shot instant

marks in seconds counted from the shot instant. The smallest distance was 14.8 km, the largest 134.8 km. From 14.8 to 99.8 km the available recording time on average was 8.0 s, from 99.8 km on up to 22.0 s.

The records were obtained as follows (Sollogub and Chekunov, 1972): low frequency apparatus SSR-30/60-KMgW and magnetic tape recording units 'Poisk48' were used together with seismographs Spen 1 (natural frequency 10–11 Hz) and NS-3 (natural frequency about 4 Hz, manufacturer unknown, perhaps home made). One recording unit consisted of a central unit and a 5.2 km long cable with vertical geophones placed every 100 m. According to the information available, usually 2 such spreads were used together, occasionally 3–4 in areas of difficult access thus allowing the recording of a total spread length of 10.4 and 20.8 km respectively. The recorded frequency band was fairly narrow with a dominant frequency of 10 Hz.

Shots were fired in boreholes 25 to 30 m deep. For longer recording distances 500–700 kg, or under unfavourable conditions 1.0–1.5 tons of explosives were used. In general not more than 50 kg TNT or 150–200 kg gunpowder were fired in one borehole. For bigger shots a cluster of boreholes was used. Shotpoint 0.0 was situated near Nogaisk on the southern boundary of the Ukrainian shield. The first 70 km of the profile crossed an Archean acidic complex. From 70 to 90 km distance migmatites, injected gneisses and contaminated granites were crossed. The rest of the profile was situated in Oligocene and Miocene formations.

To facilitate processing and presentation in reduced-time-record sections the data were digitized on a digitizing table. To reduce work only every other trace was digitized. If traces could not be followed over their full length due either to bad photographic exposure or to instrumental failures, they were omitted. Thus the average spacing on the record sections presented here is 200 m (Fig. 3). Because of failures in the original data – bad exposure, changes in time scale – together with mechanical errors associated with hand digitizing, an error of up to 0.1 s over the full length of a trace resulted.

Because the maximum recording distance was 135 km, mainly reflected and refracted waves from the crust and the crust-mantle boundary could be expected.

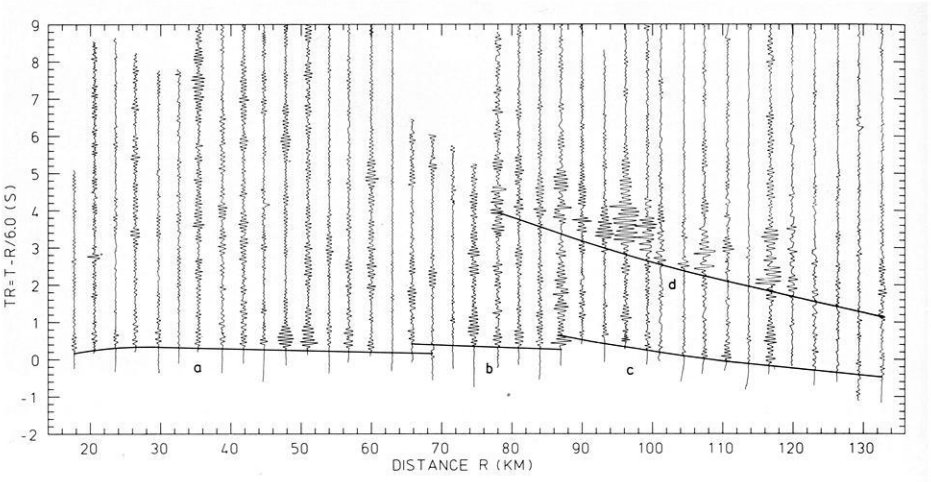

Fig. 4. Record section with mean spacing of 3 km. *a*, *b*, *c*: different branches of P_g-waves, penetrating into the basement. *d*: reflections from the crust mantle boundary ($P_M P$)

Therefore, a reduction velocity of 6.0 km/s has been chosen as this represents a good approximation for the mean crustal velocity (Fig. 3).

Correlation of Phases

In Figs. 4–6 record sections are presented with respectively 3.0, 1.0, and 0.2 km spacing between traces. Figure 4, which corresponds in observation density to record sections usually obtained in explosion seismic studies in western countries, shows a relatively simple wave-field consisting of two main phases: first arrivals that result from waves penetrating into the basement, henceforth referred to as P_g, and strong later arrivals between 75 and 135 km distance, produced by reflected waves from the Mohorovičić-discontinuity ($P_M P$). In a record section like this the first arrivals would probably be correlated in three branches as indicated in Fig. 4. Because there appear no correlatable phases between these three branches and $P_M P$ (though there are pulses of strong energy), no structure in the middle crust can be modelled.

Looking at Fig. 5, a different picture arises: a rather inhomogeneous wave-field now appears between $P_M P$ and P_g (still broken up into three parts). Fairly strong amplitudes can be followed over longer distances, interrupted only by small gaps. Relying on these data alone, one could be tempted to correlate phases over those gaps, since one could argue that these are simply due to local amplitude minima resulting, for example, from destructive interferences or high attenuation along the wave path. This is often done on wider spaced data where phases are connected over large gaps and assumed to be continuous (Fig. 5). This correlation suggests the existence of a reflector of considerable lateral extent in the middle crust.

Figure 6, however, reveals a still more complicated wave field in which seismic energy can be correlated only over short distances between P_g and

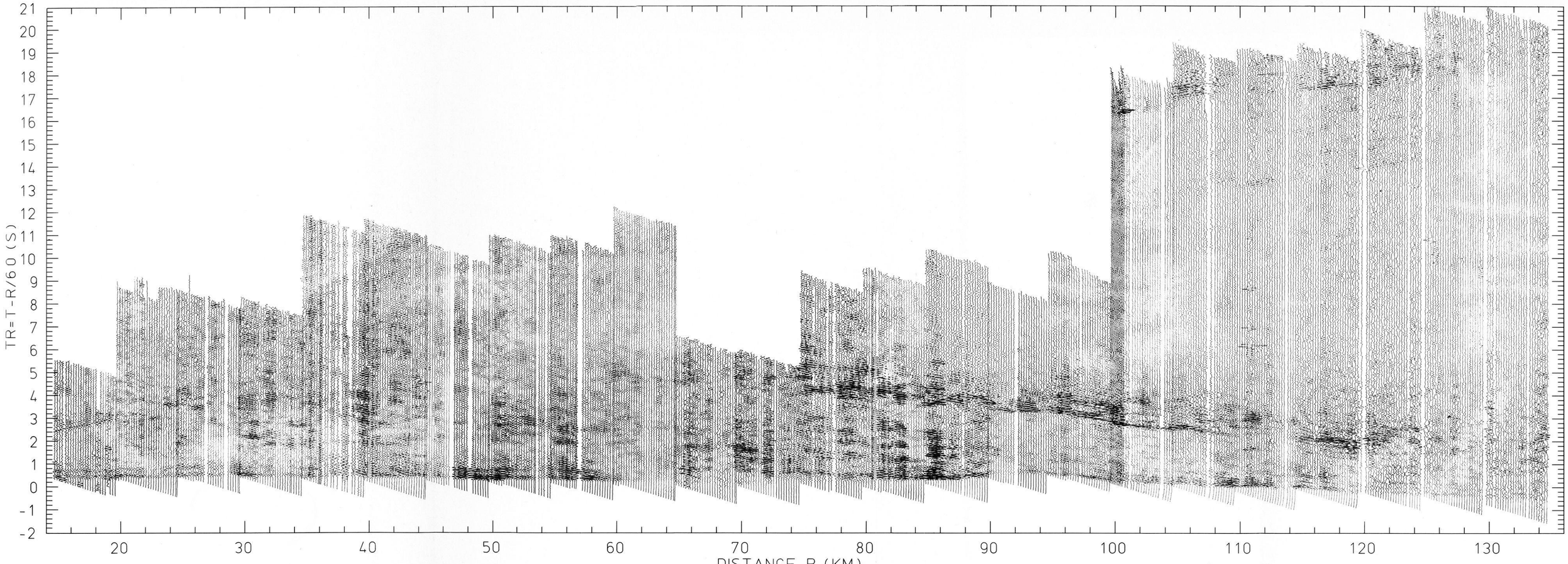

Fig. 3. Record section after handdigitizing in reduced time scale. Reduction velocity 6 km/s, mean spacing of traces 200 m

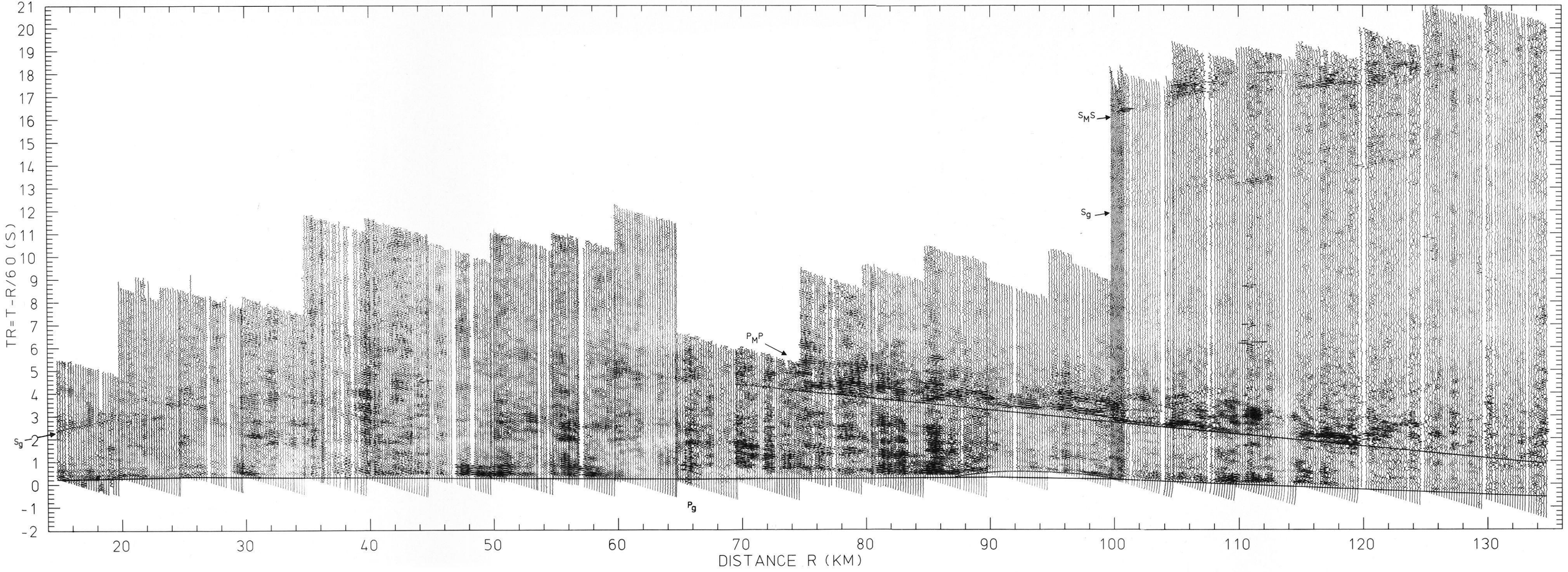

Fig. 7. Complete record section (see Fig. 3) with correlations as used for the interpretation (*solid lines*). The corresponding *S*-waves are indicated by *arrows*

$P_M P$. Such arrivals could arise from lateral inhomogeneities that are able to focus energy into certain distance ranges, and may be only of limited lateral extent. Because first arrivals appear in the gaps between 60 and 70, and 90 and 92 km distance, which led to the division into three branches in Figs. 4 and 5, P_g is correlated now as one continuous branch. These arrivals can be identified quite clearly, although the amplitudes are rather small.

The fine structure between P_g and $P_M P$ just described cannot be interpreted with the methods available, and it must be questioned of any presently available method, including two dimensional modelling would be capable of modelling structures that could be responsible for such wave patterns. Thus only the main traveltime branches have been used for the interpretation (Fig. 7).

Interpretation

Modelling was done in the following way: first traveltimes that were identified from the correlations made on the digitized record sections were read from the original data. These were then fitted by theoretical traveltime branches calculated from velocity-depth functions by trial and error. The best fitting models were then used to calculate synthetic seismograms with the reflectivity method (Fuchs, 1968; Fuchs and Müller, 1971; Müller and Kind, 1976). The computed amplitude ratios $P_g/P_M P$ were compared to the observed ratios. If no satisfying fit within the range of scatter between the observed and synthetic amplitude ratios could be obtained, the whole procedure was repeated. Amplitudes were measured from peak to peak at the maximum in a time window of 0.5 s after the respective arrival time. The distance of critical reflection of the phase $P_M P$ has been assumed to be around 75 km distance from the shotpoint since large amplitudes are observed slightly beyond this range as one would expect for the critical distance.

Two models were derived (Figs. 8a and 9a). The velocity-depth functions are listed in the appendix. Both velocity-depth functions start with 5.5 km/s

Fig. 5. Record section with mean spacing of 1 km. Branches *a, b, c, d* as in Fig. 3. Note the appearance of travel-time branches between 1 and 4s reduced time indicating structure in the middle crust

Fig. 6. Record section with mean spacing of 200 m. P_g now appears as one continuous branch. Traveltime branches between 1 and 4s reduced time now only have small horizontal persistence. *Dotted line* between 88 and 100 km corresponds to delays due to the deposits in a small sedimentary basin

Fig. 8. **a** Velocity depth function of model P2. **b** traveltimes as calculated from model P2 (*solid lines*). Small crosses indicate observed arrivals. **c** synthetic seismograms as calculated from model P2; *M* multiple reflections from the upper crust; *N* numerical effects not corresponding to real phases. **d** amplitude ratios $P_g/P_M P$. Squares and *solid line*: theoretical values as measured from 8c; *triangles*: observed ratios of peak to peak amplitudes measured at the maximum in a 0.5 s time window

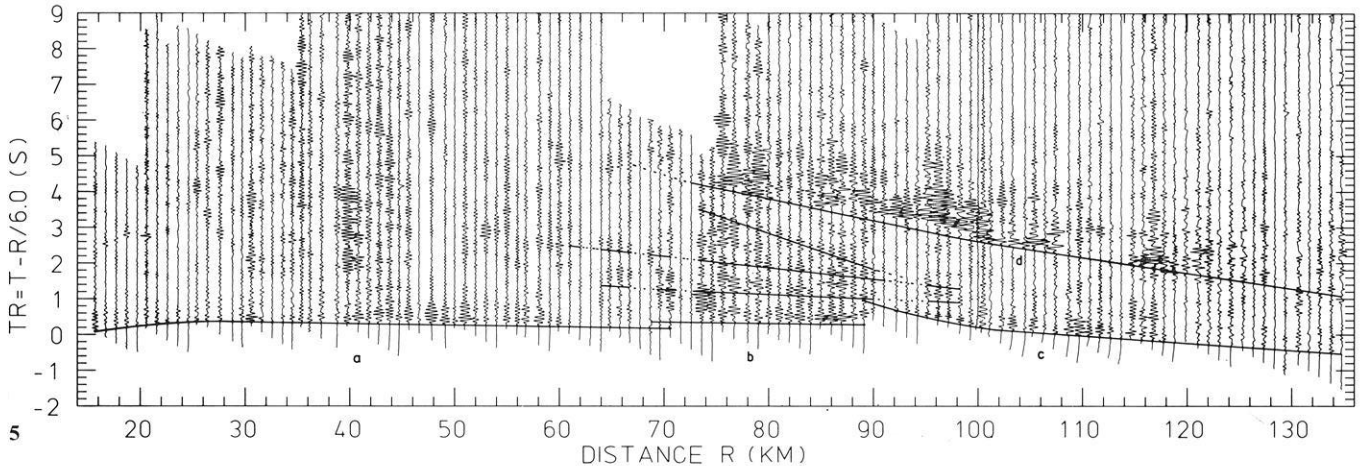

5

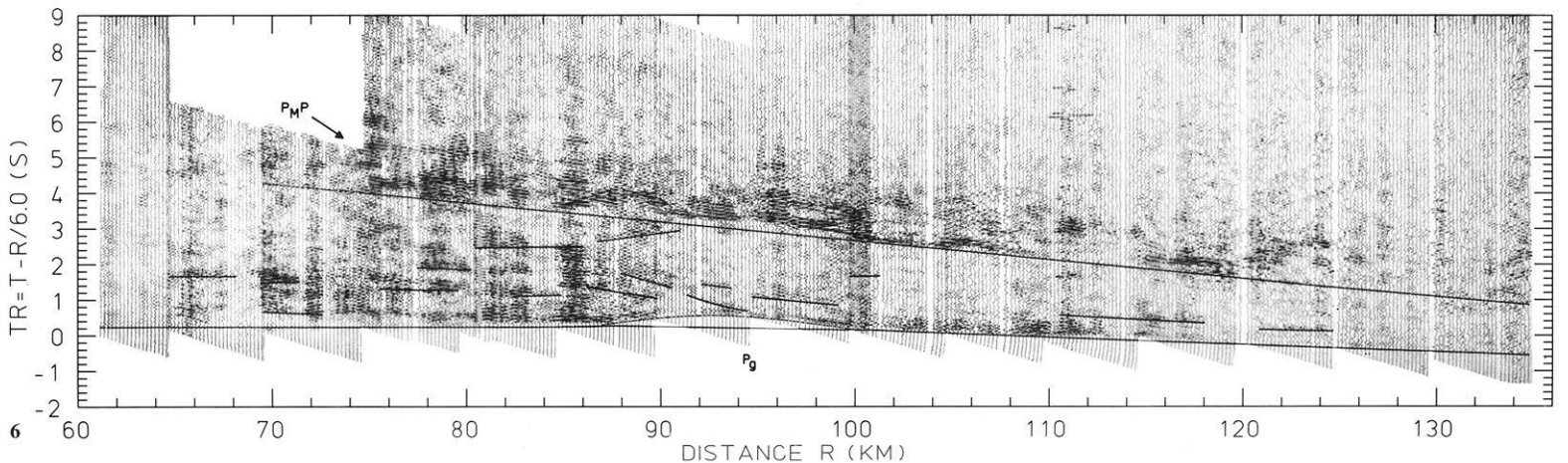

6

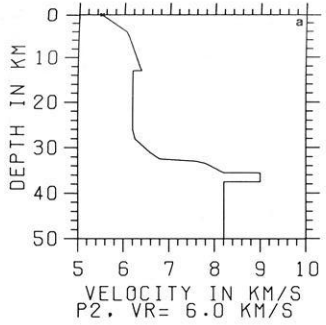
a
DEPTH IN KM
0
10
20
30
40
50
5
6
7
8
9
10
VELOCITY IN KM/S
P2. VR= 6.0 KM/S

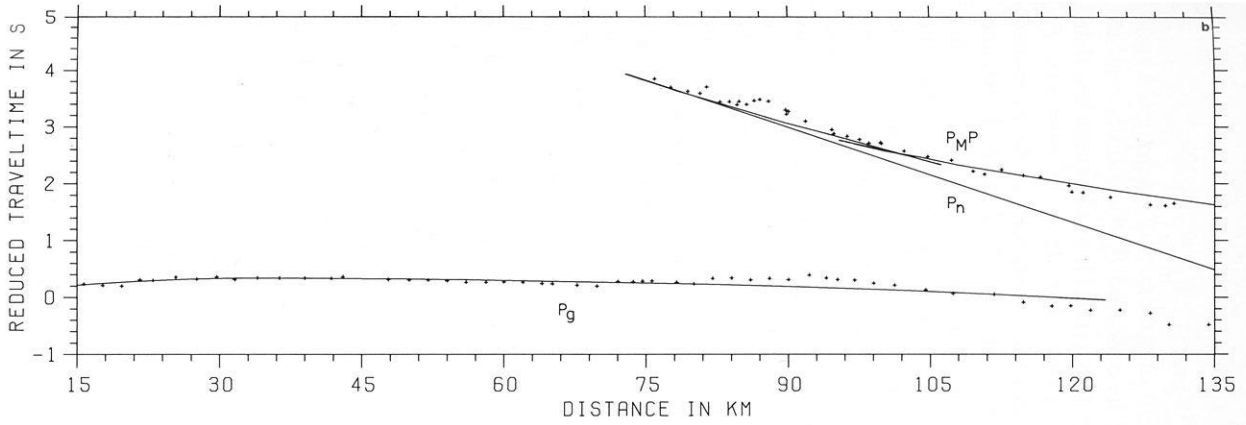
b
REDUCED TRAVELTIME IN S
5
4
3
2
1
0
-1
P_MP
P_n
P_g
15
30
45
60
75
90
105
120
135
DISTANCE IN KM

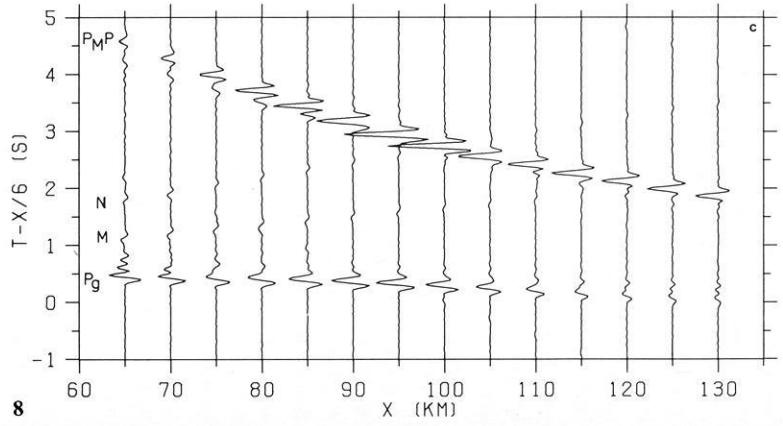
c
T-X/6 (S)
5
4
3
2
1
0
-1
P_MP
N
M
P_g
60
70
80
90
100
110
120
130
X (KM)

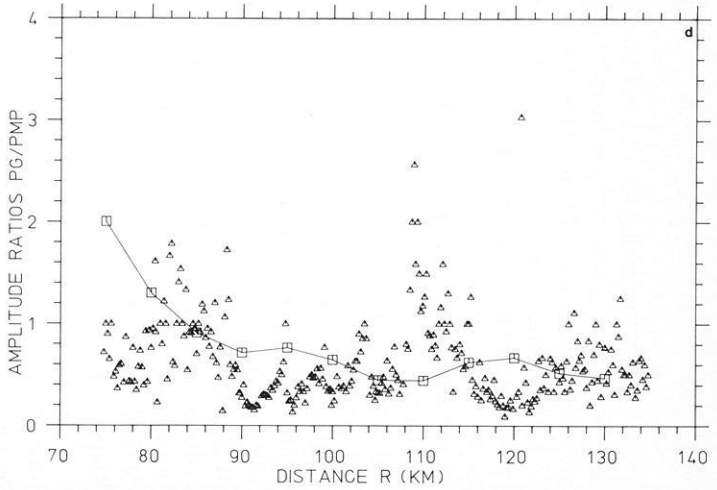
d
AMPLITUDE RATIOS PG/PMP
4
3
2
1
0
70
80
90
100
110
120
130
140
DISTANCE R (KM)

at the surface increasing to 6.1 km/s at a depth of 5.0 km and reaching 6.4 km/s at 13 km depth. These two gradients explain the observed P_g traveltimes reasonably well (Fig. 8b and 9b). Since there were no data available at distances less than 15 km, 5.5 km/s was taken as the surface velocity. The delay of observed P_g traveltimes of 0.2 s between 85 and 100 km shotpoint distance can be explained by the lower velocities in a small sedimentary basin. As $P_M P$ arrivals beyond 75 km were considered as overcritical two major problems arose: first the rather high apparent velocities of 8.8 km/s measured in the critical distance range and the resulting curvature of the $P_M P$ branch had to be explained, and secondly the amplitude ratios $P_g/P_M P$ had to be interpreted. This could be done by finding a model that produced small P_g amplitudes and large $P_m P$ amplitudes at the same time. Although the data contain no evidence for a low-velocity layer, in model P2 a small velocity decrease (6.4–6.2 km/s) was introduced at 13 km depth extending to 29.6 km so as to enable P_g amplitudes to be reduced to match the observed ratios $P_g/P_M P$ (Figs. 8c and d). This could not be done at will (for example by decreasing the depth of the upper boundary of the low-velocity layer) because there are significant P_g arrivals beyond 100 km distance in the observations that cannot be ignored. Thus $P_M P$ amplitudes had to be modelled large enough. One possibility to do so and at the same time to explain the curvature of the $P_M P$-traveltime branch would have been simply to increase the upper mantle velocity. This velocity could in principle be checked by the P_n arrivals. Unfortunately, the observation range of 135 km on this profile was not long enough to observe P_n as first arrival. Second arrivals within the observation range that could be identified as P_n (for example by being tangential to $P_M P$ or having a high velocity) were also not observed. Thus an explanation had to be found for the large amplitudes and the curvature of the $P_M P$-traveltime branch that would not result in a headwave with strong second arrivals tangential to $P_M P$ or with a correspondingly high velocity in the synthetic seismograms. This problem was solved by introducing a thin layer of high velocity immediately beneath the Moho (Fuchs and Schulz, 1976). The thickness of this layer has been chosen to be one wavelength. Other thicknesses were tried, but no significant changes in amplitudes arose. The thickness of one wavelength is sufficient to suppress P_n in the synthetic seismograms in agreement with the observations.

The Moho itself was modelled as a broad transition zone at which the velocity increases from 6.4 to 8.2 km/s. This was suggested by the absence of PS/SP converted waves in the observations at about twice the reduced $P_M P$-arrival times where one would expect such waves (Fig. 7). A first order discontinuity could also explain the observed traveltimes of $P_M P$ but at the same time would produce such conversions with considerable amplitudes whereas a transition zone suppresses them (Fuchs, 1975). Although the upper boundary of the high-velocity layer is a first order discontinuity no PS conversions arise, because the velocity contrast with respect to the overlying layer (0.8 km/s) is not strong enough. A 2 km/s contrast would have been necessary to produce PS conversions (Fuchs, 1975).

Thus a fit of the observed amplitude ratios was obtained within the range of scatter (Fig. 8d). Only beyond 120 km distance the computed ratios are too low because of the shadow zone resulting from the crustal low-velocity

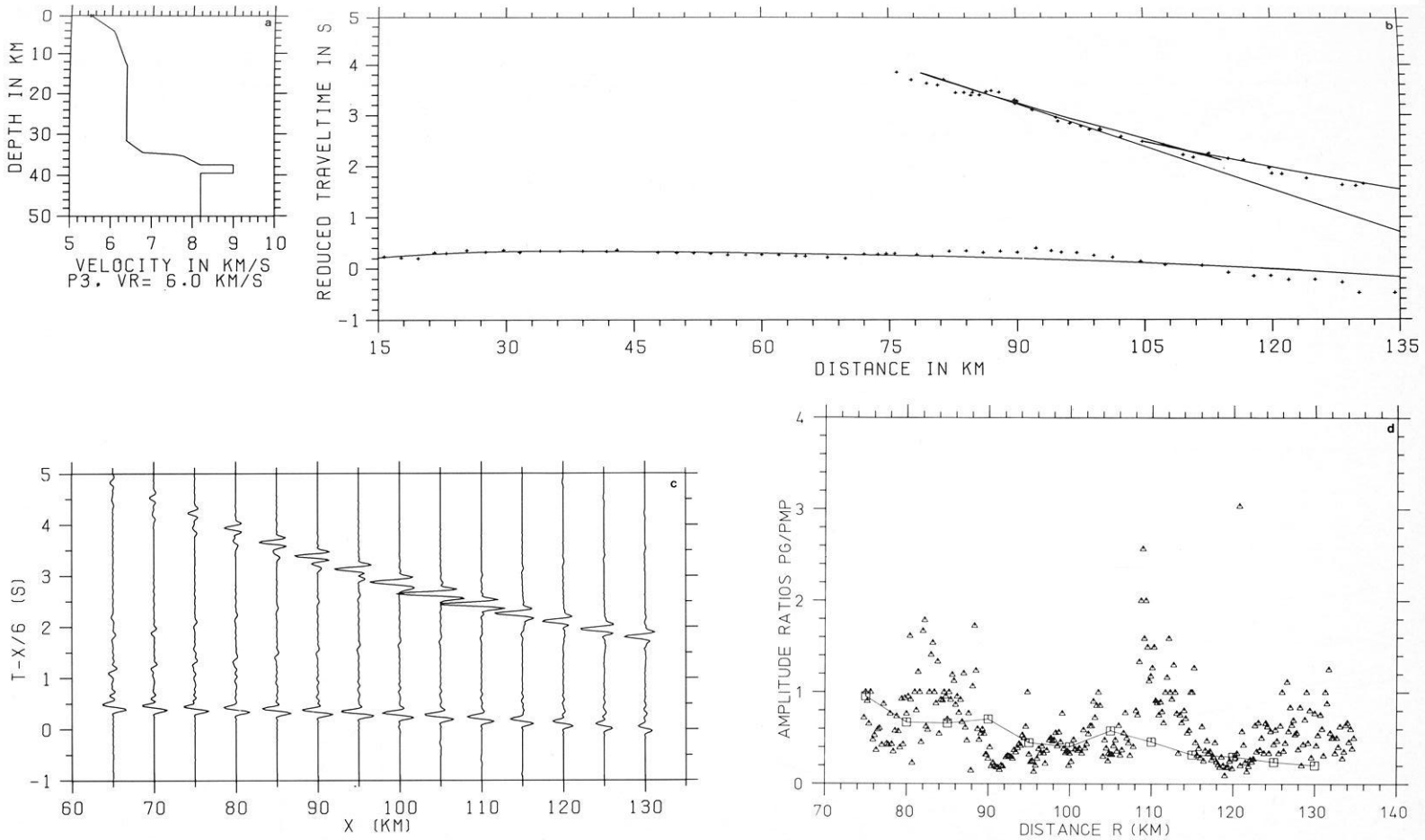

Fig. 9a–d. Same as Fig. 8, now for model P3

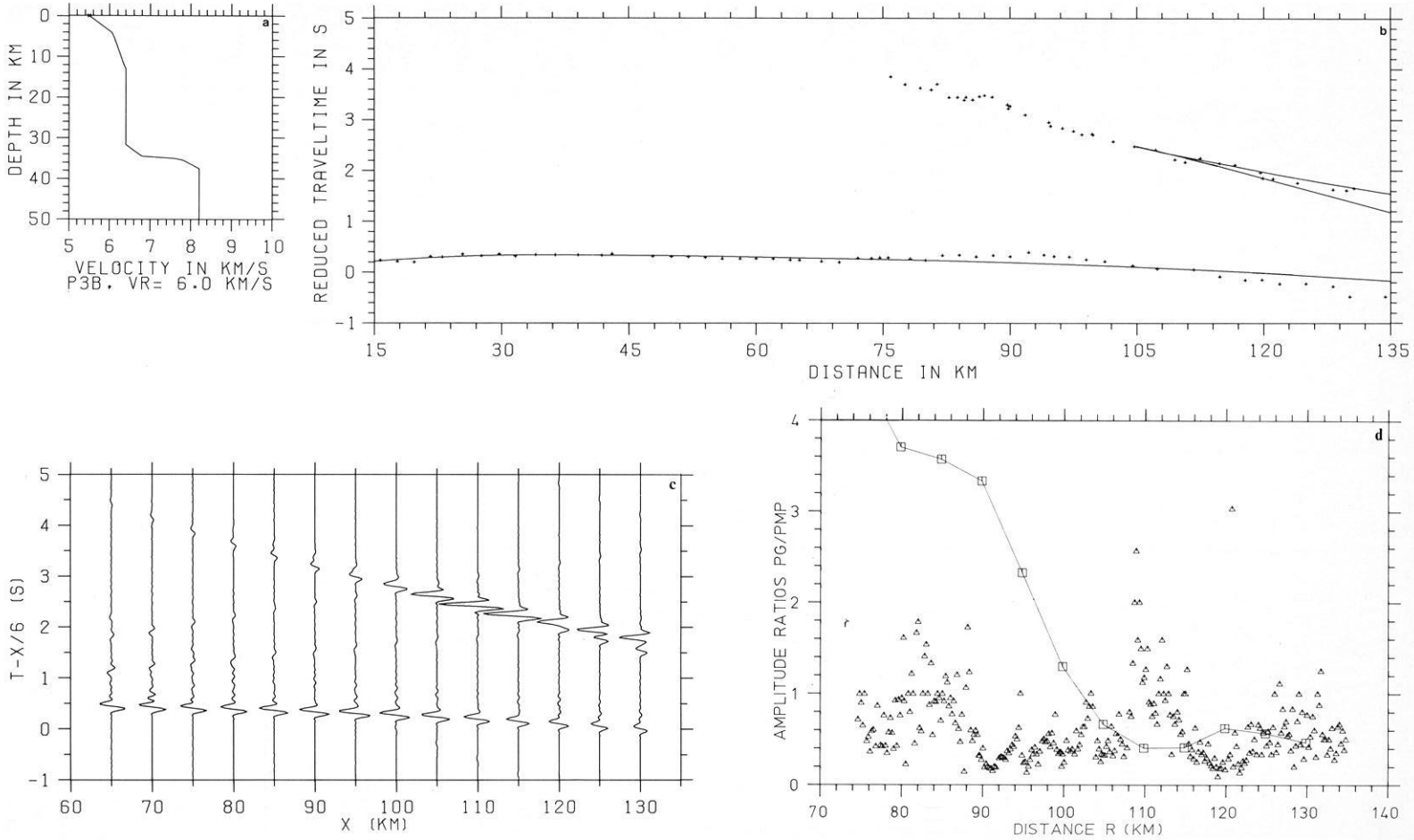

Fig. 10a–d. Same as Fig. 8, now for model P3B. Note the fast drop of amplitudes in the critical distance range between 100 and 105 km due to omitting the high velocity layer

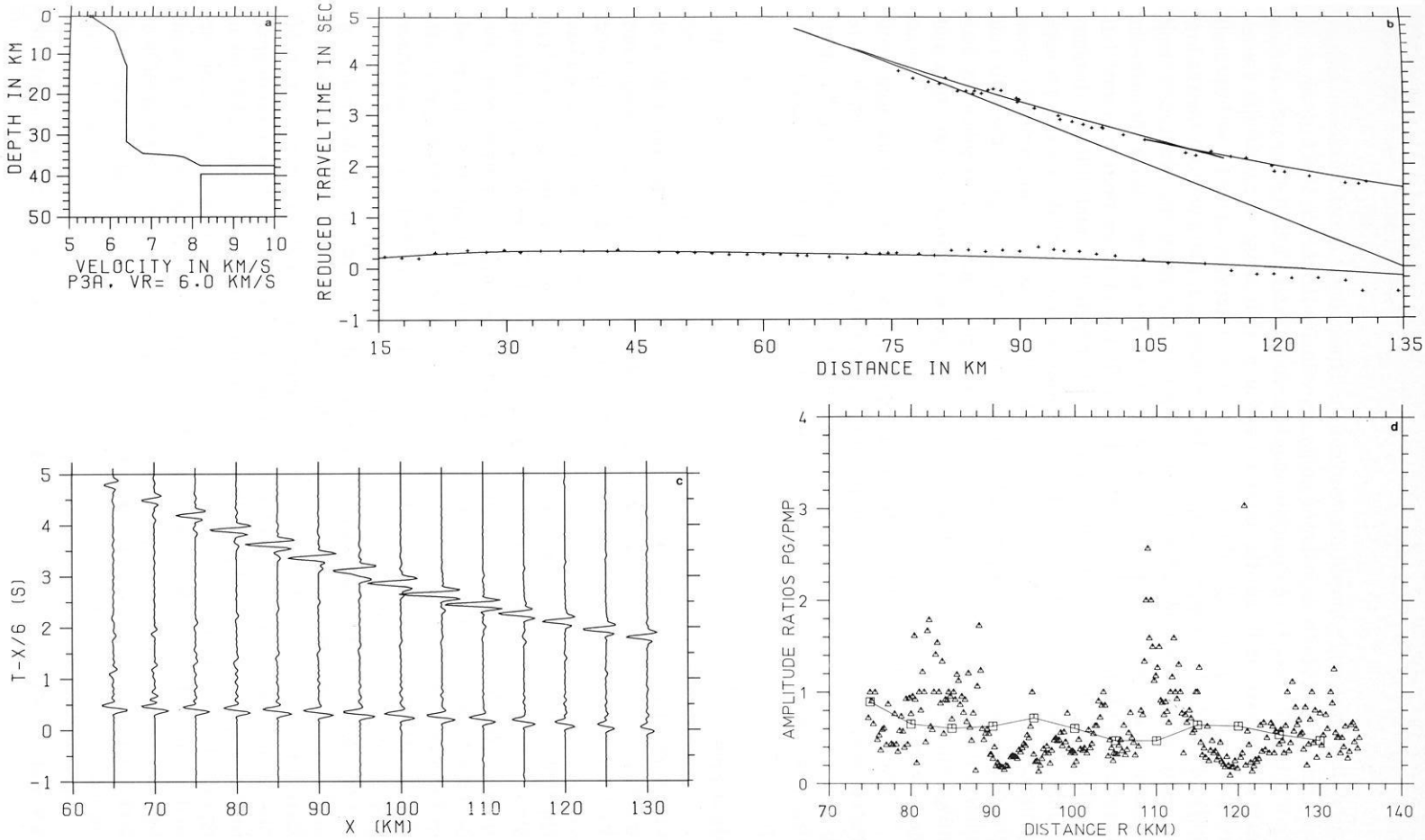

Fig. 11a–d. Same as Fig. 8, now for model P3A showing the effect of an extreme high velocity (10 km/s right beneath the crust mantle boundary)

zone that reduces P_g amplitudes too much. Thus, this zone of reduced velocity has been replaced by a layer of constant velocity down to 31.6 km depth in model P3 (Fig. 9a). Here P_g amplitudes between 70 and 100 km increase resulting in a slightly worse fit of the observed ratios in that range. Because the scatter of the data is quite high, this fit may also be tolerated. The fit is improved beyond 100 km because P_g amplitudes become stronger there without the shadow zone caused by the low-velocity layer (Fig. 9c). The fit of the observed traveltimes became slightly worse because of the 6.4 km/s velocity. With the gradient reaching 6.7 km/s at 18 km depth a better fit would have been obtained but at the same time too large P_g amplitudes between 100 and 120 km distance would have resulted. Therefore, 6.4 km/s must be considered as a compromise between the two solutions. As there is no delay due to a low-velocity layer the depth of the Moho transition increases by 2 km. In Fig. 10 the effect of omitting the high-velocity layer is demonstrated. Figure 11a–d gives an idea how a maximum velocity of 10 km/s would change the theoretical traveltime and amplitude curves.

Other possibilities like a stack of thin lamina or a low-velocity zone with higher velocity contrast at the upper boundary, situated at greater depth, were not able to explain the amplitude ratios and the curvature of the $P_M P$ branch in the critical region with 'normal' sub-Moho velocities of 8.0–8.2 km/s.

Discussion

At this point the question must be raised as to what extent the models derived in this paper resemble the real structure of the earth. Already the correlations shown in Figs. 4–7 reflect the problems one has to face in interpreting refraction seismic data. Apart from the fact that picking of secondary onsets and phases depends highly on the observer's opinion, even with narrow spaced data where one might think that waves correlate automatically the large number of short-running phases reflected from the middle crust is hard to interpret with the methods available today. The methods used for this interpretation are based on the assumption that the earth consists of homogeneous horizontal layers of large extent. If one considers the highly disturbed and heterogeneous surface geology one must allow for similar structures in the deeper parts of the crust so that flat layering over large distances will be a strong simplification of reality. Where energy is correlatable over large distances, however, such a lateral continuity seems to in fact be present underground, and an interpretation of these phases like the one presented here seems to be justified. The velocity-depth functions of models P2 and P3 between 13 km and, respectively, 29.6 and 31.6 km depth (Figs. 8 and 9), will be too simple to reflect the true structure of the earth in these depths. The velocity-depth function above 13 km depth has been derived from the assumption that P_g is a continuous branch, as described earlier. Slight changes could arise if one preferred the first arrivals to be split into more than one traveltime branch.

The range of possible models that satisfy the data excludes the possibility of a sharp discontinuity at the crust-mantle boundary and indicates a smooth

transition zone. If one would be more inclined to omit the high velocity layer by defining the critical point at larger distances (beyond 110 km) one could explain the traveltimes with 'normal' Moho velocities around 8.0 km/s but would then have to face the facts that the large amplitudes around 75 km distance could not be explained.

Because the use of amplitudes had a major influence on the models presented here, the question arises as to whether this is really justified. With the use of amplitude ratios one would expect a reduction of the scatter that usually is imposed on the normal amplitude-distance graphs, because the effects of surface geology near the shotpoint and the receivers will be eliminated. In Figs. 8d–11d, however, still much scatter appears, so that the theoretical curves only represent one possibility within a whole family of solutions. This is mainly due to the sensitivity of the high frequency signals of this set of data to horizontal and vertical inhomogeneities within the crust. Thus, it must be questioned as to whether amplitude information can really improve results gained from traveltimes in such high-frequency studies. The two main points affected by the consideration of amplitudes in models P2 and P3 are the following:

Firstly, the 6.4 km/s velocity at 13 km depth would have been increased to 6.7 km/s at 18 km depth, which would explain the observed traveltimes beyond 110 km distance much better and would possibly represent a better estimate for a velocity in such depths in a stable shield area (Berry and Fuchs, 1973; Hirschleber et al., 1975). The only reason why it has been omitted was that the synthetic $P_g/P_M P$ ratios computed from it would not fit the observed ones. Secondly, the maximum velocity of 9 km/s immediately beneath the Moho would have been replaced by normal values of maximum 8.2–8.3 km/s which still would explain $P_M P$ traveltimes, but would lead to smaller amplitudes at distances less than 80 km – thus the introduction of the high velocity layer was necessary.

In comparison with the interpretations of profile 10 of Pavlenkova and Smelyanskaya (1970) and Pavlenkova (1971) the following differences and similarities can be stated: two different models, one with and one without a low-velocity zone (Figs. 12a and b) have been obtained. The P_g traveltime branch that was correlated as one continuous curve here has been broken up into several branches (Pavlenkova, 1973) which leads to two main reflectors in the two-dimensional models between 10 and 20 km depth, whereas a rather smooth gradient without a distinct reflector appears in the models P2 and P3 (Figs. 8a and 9a) down to 13 km depth (these models would correspond to a depth section at about 60 km distance in Fig. 12). The phases of short horizontal persistence that appear between 1 and 4 s reduced time in the record sections (Fig. 6) have been interpreted in terms of small and sometimes steeply inclined reflectors in the middle crust (10–25 km depth) in the earlier published interpretations (Fig.12) whereas no attempt has been made in the present paper to find explanations for those phases because the analysis methods were not suitable to do so. One has to ask, whether such a complicated wavefield which definitely indicates a very complicated crustal structure can really be interpreted with presently available techniques even if more data of the same quality as the ones presented here were available. From the data available here it was not

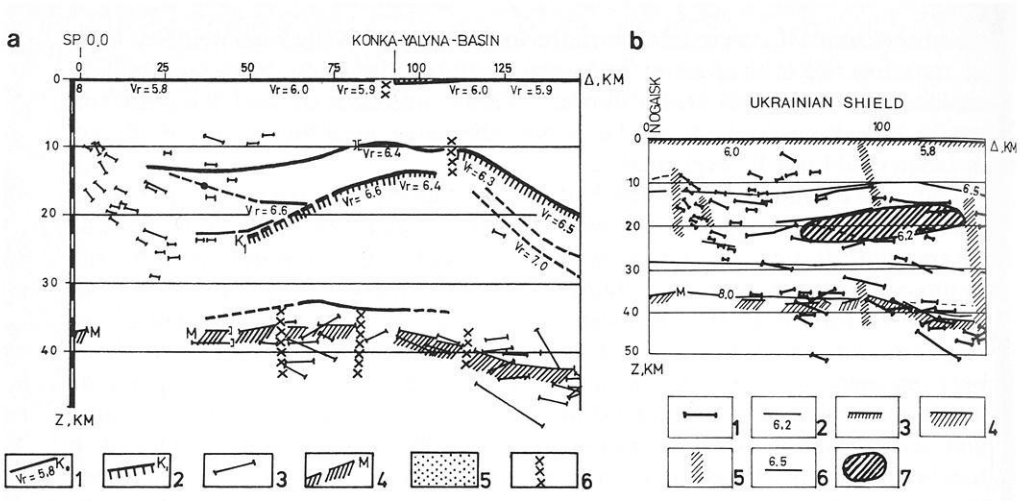

Fig. 12a and b. Different interpretations of the part of profile 10 covered by shot 0.0. **a**: crystalline basement surface with velocities in km/s; 2: Conrad surface; 3: reflectors; 4: Moho; 5: sedimentary layer; 6: disjunctive dislocations. (Modified from Sollogub and Chekunov, 1972) **b**: 1: reflectors; 2: refractors with boundary velocities in km/s; 3: crystalline basement surface; 4: Moho; 5: deep reaching faults; 6: lines of iso velocity; 7: low velocity zone; (modified from Pavlenkova, 1973)

possible to decide if a low velocity layer is really present on this part of the Ukrainian shield. Also the earlier published interpretations allow for the two possibilities (Alekseev et al., 1973). The crust-mantle boundary as a horizontally and vertically heterogeneous zone with a system of criss-crossing, inclined reflectors and refractors has been derived from the complicated wavefield of the $P_M P$-reflection (Fig. 7) by Pavlenkova and Smelyanskaya (1970). Since the phases appear in a complicated but somewhat regular pattern with large amplitudes and show up on reversed and overlapping profiles also, they are assumed to originate from the same depth range. The possibility that the heterogeneous structure of the overlying crust is responsible for this $P_M P$-pattern was ruled out by the argument that other phases do not show similar features as the $P_M P$ reflections. This may be a bit too rigorous, though, because from the wavefield between P_g and $P_M P$ (Fig. 6) which also shows a somewhat regular pattern with pulses of high energy and from similar detailed studies (Healy, 1971) one has to ask why mid-crustal structure should have no effect on waves reflected from the base of the crust.

The transition zone at the Moho as presented in this paper has been derived from the absence of PS-SP converted waves. The maximum velocity is 8.2 km/s and is reached at approximately the same depth as the 8.0 km/s velocity in Fig. 12a and b. In summary the models P2 and P3 show the same main structures as the two-dimensional solutions of Fig. 12 with the exception of the high velocity layer which has to be treated with caution anyway, because it is based on amplitude data alone.

As a result it seems sensible to record at station intervals of 100–200 m only if a great many overlapping, crossing and reversed profiles are measured

so that a better control over the crustal structure is obtained, and if much more sophisticated methods can be developed to handle such data. With high quality data and some care applied to the correlations a station spacing of 1–2 km seems to be sufficient to achieve reasonable results.

Acknowledgements. I am indebted to Professor Dr. K. Fuchs for making this work possible and for stimulating discussions. My special thanks go to Dr. Kind who was always there for discussions, advice and help. The data was kindly provided by Drs. Sologub and Pavlenkova. Drs. C. Prodehl, G. Müller, and D. Bamford critically read the manuscript. The calculations were performed at the Rechenzentrum der Universität Karlsruhe and on the RAYTHEON 500 of the Geophysical Institute Karlsruhe.

Appendix

Model P2		Model P3	
z (km)	v_p (km/s)	z (km)	v_p (km/s)
0.0	5.5	0.0	5.5
4.0	6.0	4.0	6.0
5.0	6.1	5.0	6.1
12.0	6.3	12.0	6.3
13.0	6.4	13.0	6.4
13.0	6.2	31.6	6.4
26.0	6.2	33.0	6.6
29.6	6.4	34.5	6.8
31.0	6.6	35.0	7.6
32.5	6.8	35.4	7.8
33.0	7.6	37.5	8.2
33.4	7.8	37.5	9.0
35.5	8.2	39.5	9.0
35.5	9.0	39.5	8.2
37.5	9.0		
37.5	8.2		

Model P3A like P3, maximum velocity at the high velocity layer is 10 km/s
Model P3B like P3 up to 37.5 km depth, then halfspace with velocity 8.2 km/s

References

Alekseev, A.S., Belonosova, A.V., Burmakov, I.A., Krasnopevtseva, G.V., Matveeva, N.N., Nersessov, G.L., Pavlenkova, N.I., Romanov, V.G., Ryaboi, V.Z.: Seismic studies of low-velocity layers within the crust and upper mantle on the territory of the USSR. Tectonophysics **20**, 47–56, 1973

Berry, M.J., Fuchs, K.: Crustal structure of the superior and Greenville provinces of the northeastern Canadian Shield. Bull. Seismol. Soc. Am. **63**, 1393–1432, 1973

Fuchs, K.: Das Reflexions- und Transmissionsvermögen eines geschichteten Mediums mit beliebiger Tiefenverteilung der elastischen Moduln und der Dichte für schrägen Einfall ebener Wellen. J. Geophys. **34**, 389–413, 1968

Fuchs, K.: Synthetic seismograms of Ps-reflections from transition zones computed with the reflectivity method. J. Geophys. **43**, 445–462, 1975

Fuchs, K., Müller, G.: Computation of synthetic seismograms with the reflectivity method and comparison with observations. Geophys. J. R. Astron. Soc. **23**, 417–433, 1971

Fuchs, K., Schulz, K.: Tunneling of low frequency waves through the subcrustal lithosphere. J. Geophys. **42**, 175–190, 1976

Healy, J.H.: A comment on the evidence for a worldwide zone of low seismic velocity at shallow depths in the earth's crust. In: The structure and physical properties of the earth's crust, Geophysical Monograph 14, Heacock (ed.), pp. 35–40. Washington, D.C.: American Geophysical Union 1971

Hirschleber, H.B., Lund, C.-E., Meissner, R., Vogel, A., Weinrebe, W.: Seismic investigations along the Scandinavian 'Blue Road' traverse. J. Geophys. **41**, 135–148, 1975

Kosminskaya, I.P.: Deep seismic sounding of the earth's crust and upper mantle. Special report, Consultants Bureau, London 1971

Müller, G., Kind, R.: Observed and computed seismograms for the whole earth. Geophys. J.R. Astron. Soc. **44**, 699–716, 1976

Pavlenkova, N.I.: Methods and some results of velocity-cross-section determination for the earth's crust in the Ukraine, I and II. Geofiz. Sb. **39**, 12–22 and **42**, 46–55, 1971

Pavlenkova, N.I.: Elastische Wellen und Modelle der Erdkruste (in Russian). Kiev, 1973

Pavlenkova, N.I., Smelyanskaya, T.V.: The nature of the group of reflected waves from the base of the earth's crust. Izv., Physics of the solid earth 10–18, 1970

Sollogub, V.B., Chekunov, A.V.: The results of DSS measurements in the Ukrainian Soviet Socialist Republic. In: The crustal structure of Central and Southeastern Europe based on the results of explosion seismology, Hungarian Geophysical Institut 'Roland Eötvös', Geophysical Transactions, Special Edition. Budapest: Muszaki Könyokiado 44–68, 1972

Sollogub, V.B., Litvinenko, I.V., Chekunov, A.V., Ankudinov, S.A., Ivanov, A.A., Kalyuzhnáya, L.T., Kokorina, L.K., Tripolsky, A.A.: New DSS-data on the crustal structure of the Baltic and Ukrainian Shields. Tectonophysics **20**, 67–84, 1973a

Sollogub, V.B., Prosen, D., Dachev, C., Petkov, I., Velchev, T., Andonova, E., Mihailov, S., Mituch, E., Posgay, K., Militzer, H., Knothe, C., Uchman, I., Constantinescu, P., Cornea, I., Subbotin, S.I., Chekunov, A.V., Garkalenko, I.A., Khain, V.E., Slavin, V.I., Beranek, B., Weiss, J., Hridlička, A., Dudek, A., Zounkova, M., Suk, M., Feifar, M., Milovanović, B., Roksandić, M.: Crustal structure of central and southeastern Europe by data of explosion seismology. Tectonophysics **20**, 1–33, 1973b

Received June 30, 1978; Revised Version March 10, 1979; Accepted May 9, 1979